

Salicylic Acid–Independent ENHANCED DISEASE SUSCEPTIBILITY1 Signaling in *Arabidopsis* Immunity and Cell Death Is Regulated by the Monooxygenase *FMO1* and the Nudix Hydrolase *NUDT7*^W

Michael Bartsch,^a Enrico Gobbato,^a Pawel Bednarek,^a Svenja Debey,^b Joachim L. Schultze,^b Jaqueline Bautor,^a and Jane E. Parker^{a,1}

^aDepartment of Plant–Microbe Interactions, Max Planck Institute for Plant Breeding Research, D-50829 Cologne, Germany

^bMolecular Tumor Biology and Tumor Immunology, Clinic I, University of Cologne, D-50937 Cologne, Germany

***Arabidopsis thaliana* ENHANCED DISEASE SUSCEPTIBILITY1 (EDS1) controls defense activation and programmed cell death conditioned by intracellular Toll-related immune receptors that recognize specific pathogen effectors. EDS1 is also needed for basal resistance to invasive pathogens by restricting the progression of disease. In both responses, EDS1, assisted by its interacting partner, PHYTOALEXIN-DEFICIENT4 (PAD4), regulates accumulation of the phenolic defense molecule salicylic acid (SA) and other as yet unidentified signal intermediates. An *Arabidopsis* whole genome microarray experiment was designed to identify genes whose expression depends on EDS1 and PAD4, irrespective of local SA accumulation, and potential candidates of an SA-independent branch of EDS1 defense were found. We define two new immune regulators through analysis of corresponding *Arabidopsis* loss-of-function insertion mutants. FLAVIN-DEPENDENT MONOOXYGENASE1 (FMO1) positively regulates the EDS1 pathway, and one member (NUDT7) of a family of cytosolic Nudix hydrolases exerts negative control of EDS1 signaling. Analysis of *fmo1* and *nudt7* mutants alone or in combination with *sid2-1*, a mutation that severely depletes pathogen-induced SA production, points to SA-independent functions of FMO1 and NUDT7 in EDS1-conditioned disease resistance and cell death. We find instead that SA antagonizes initiation of cell death and stunting of growth in *nudt7* mutants.**

INTRODUCTION

Plants have evolved multiple layers of cellular innate immunity for protection against pathogen infection (Nürnberger et al., 2004; Lipka et al., 2005). An important defense layer (known as basal resistance) is expressed in response to invasive pathogens and serves to restrict their growth and the progression of disease (Glazebrook, 2005). Basal resistance depends on the timely activation of defense pathways and can be potentiated by receptors recognizing conserved pathogen-associated molecular patterns or specific pathogen effectors (Belkhadir et al., 2004; Nürnberger et al., 2004; Glazebrook, 2005).

Pathogen effector recognition by specialized immune receptors (known as Resistance [R] proteins) is normally associated with a localized burst of reactive oxygen species (ROS) and programmed plant cell death (the hypersensitive response [HR]) at infection sites. It also causes stimulation of basal defenses involving the phenolic molecule salicylic acid (SA) (Glazebrook et al., 2003; Eulgem et al., 2004). The processes by which R

protein recognition connects to basal defense activation are unknown but are influenced by the particular receptor type. Thus, many R proteins of the nucleotide binding–leucine-rich repeat (NB-LRR) class that have N-terminal coiled-coil (CC) domains require the membrane-attached protein NONSPECIFIC DISEASE RESISTANCE1 for resistance (Aarts et al., 1998; Coppinger et al., 2004). Plant NB-LRR proteins that instead have an N-terminal Toll Interleukin1 Receptor (TIR) domain depend on the intracellular protein EDS1 and its interacting partners, PAD4 and SENESCENCE-ASSOCIATED GENE101 (SAG101) (Aarts et al., 1998; Feys et al., 2001, 2005). Significantly, the *Arabidopsis thaliana* CC-NB-LRR protein RESISTANCE TO PSEUDOMONAS SYRINGAE PV MACULICOLA1 (RPM1) conditions local programmed cell death, SA accumulation, and resistance independently of EDS1 or PAD4 but needs these regulators to transduce defense and death-promoting signals in cells surrounding pathogen infection foci (Rustérucchi et al., 2001; Wiermer et al., 2005). Therefore, RPM1, and probably other structurally related CC-NB-LRR immune receptors, engages the ENHANCED DISEASE SUSCEPTIBILITY1 (EDS1)/PHYTOALEXIN-DEFICIENT4 (PAD4) pathway even though it is not required for local resistance or cell death.

Arabidopsis EDS1 complexes are essential for basal resistance to invasive biotrophic and hemibiotrophic pathogens in the absence of R protein recognition (Zhou et al., 1998; Jirage et al., 1999; Feys et al., 2001, 2005). In both the basal and TIR-NB-LRR conditioned responses, EDS1 and its partners control production

¹ To whom correspondence should be addressed. E-mail parker@mpiz-koeln.mpg.de; fax 49-221-5062-353.

The author responsible for distribution of materials integral to the findings presented in this article in accordance with the policy described in the Instructions for Authors (www.plantcell.org) is: Jane E. Parker (parker@mpiz-koeln.mpg.de).

^WOnline version contains Web-only data.

Article, publication date, and citation information can be found at www.plantcell.org/cgi/doi/10.1105/tpc.105.039982.

of SA and other as yet undefined molecules to amplify defenses (Rustérucci et al., 2001; Eulgem et al., 2004; Song et al., 2004). Some genes that function in SA biosynthesis and signal relay have been isolated (Wildermuth et al., 2001; Nawrath et al., 2002; Dong, 2004). However, little is known about processes regulating the predicted SA-independent branch of EDS1 defense. Recent data reveal that EDS1 and PAD4 transduce ROS-derived signals in biotic and abiotic stress signaling (Rustérucci et al., 2001; Mateo et al., 2004), and this may be central to their activities beyond controlling SA (Wiermer et al., 2005).

In this study, we used *Arabidopsis* whole genome microarrays to examine the EDS1 regulatory node in disease resistance. In particular, we aimed to identify components of EDS1 signaling that are not within the SA pathway. We reasoned that the absence of effects of *eds1* or *pad4* null mutants on *RPM1*-triggered local resistance, cell death, and SA production (Feys et al., 2001; Rustérucci et al., 2001) would allow us to extract candidate genes that, beyond these events, are *EDS1* and *PAD4* dependent. Characterization of *Arabidopsis* insertion mutants in a discrete group of pathogen-responsive genes whose expression depends robustly on *EDS1* and *PAD4* resulted in identification of *FLAVIN-DEPENDENT MONOOXYGENASE1 (FMO1)* as a positive regulator and one member (*NUDT7*) of a cytosolic Nudix hydrolase family as a negative regulator of EDS1-conditioned resistance and cell death. Measurements of SA in these mutants combined with genetic analyses establish that *FMO1* and *NUDT7* are important for signaling through an EDS1-dependent but SA-independent branch of plant defense.

RESULTS

Experimental Design and Microarray Data Analysis

We used Affymetrix ATH1 GeneChips representing 22,734 *Arabidopsis* genes (Redman et al., 2004) to examine transcriptional profiles of wild-type leaves of accession Wassilewskija (*Ws-0*) and the *Ws-0* null mutants *eds1-1* and *pad4-5* before treatment and at 3 and 6 h after bacterial infiltration. A previous study revealed that *avrRpm1*-specific cellular changes are registered in cells ~3 h after bacterial infiltration (de Torres et al., 2003). Plants were either mock-inoculated with buffer (10 mM MgCl₂) or infiltrated with a high titer (10⁷ colony-forming units [cfu]/mL) of *Pseudomonas syringae* pv *tomato* (Pst) DC3000 strains expressing either *avrRpm1* (triggering *EDS1/PAD4*-independent *RPM1* resistance) or *avrRps4* (*EDS1/PAD4*-dependent *RESISTANT TO PSEUDOMONAS SYRINGAE4 [RPS4]* resistance) (Table 1). We reasoned that selection of pathogen-responsive genes whose expression was affected by both *eds1* and *pad4* null mutants would increase the likelihood of identifying genes that are robustly under transcriptional control of EDS1 and its interacting and cofunctioning partner, PAD4. A further criterion exploited the dispensability of *EDS1* and *PAD4* in *RPM1* local resistance, SA production, and programmed cell death to extract candidate genes preferentially expressed in an SA-independent branch of EDS1 signaling. Untreated wild-type and mutant material was incorporated to the experiment (Table 1) to investigate whether defects in *eds1* or *pad4* plants could be detected at the transcriptional level in pathogen-unchallenged leaves.

Table 1. Expression Microarray Sampling

Plant	Treatment ^a	Harvest (h)	HR (h) ^b
Wild type (<i>Ws-0</i>)	Nontreated	3	–
	10 mM MgCl ₂	3, 6	–
	Pst <i>avrRpm1</i>	3, 6	6
	Pst <i>avrRps4</i>	3, 6	24
<i>eds1-1</i>	Nontreated	3	–
	10 mM MgCl ₂	3, 6	–
	Pst <i>avrRpm1</i>	3, 6	6
	Pst <i>avrRps4</i>	3, 6	–
<i>pad4-5</i>	Nontreated	3	–
	10 mM MgCl ₂	3, 6	–
	Pst <i>avrRpm1</i>	3, 6	6
	Pst <i>avrRps4</i>	3, 6	24

^a Pst DC3000 expressing *avrRpm1* or *avrRps4* was infiltrated at 10⁷ cfu/mL into leaves.

^b Time of appearance of confluent HR in hours, measured by trypan blue staining. –, HR not detected within 24 h.

To ensure uniformity of plant responses and reduce experimental noise, we recorded the timing of plant cell death after bacterial treatment in each experiment, and this was found to be consistent with previous analyses (Table 1) (Rustérucci et al., 2001). Equal amounts of total RNA from three biological replicates were pooled before cRNA labeling reactions, and the cRNA probes hybridized to individual Affymetrix (ATH1) GeneChips, producing 21 data sets (Table 1). Details of computational methods to process gene expression data are described in Methods.

By comparing transcriptional profiles of pathogen- and mock-inoculated wild-type samples, we identified probe sets whose expression changed (induced or repressed) at least twofold at 3 or 6 h in at least two pathogen treatments. This defined a group of 4522 *Arabidopsis* genes as pathogen responsive (see Supplemental Table 1 online).

Definition of *EDS1/PAD4*-Regulated Genes

In this article, we focus on analysis of pathogen-inducible genes whose expression was dependent on both *EDS1* and *PAD4* in *RPM1*-conditioned responses (referred to as Group I genes). Searching for genes that were at least twofold upregulated in the wild type but had a twofold lower expression in *eds1-1* and *pad4-5* revealed a group of seven genes, including *PAD4*, as shown in Table 2. Since the microarray analysis was not replicated, we considered these genes as candidates for further analysis. The identities of Group II genes (whose expression was strongly dependent on *EDS1* and *PAD4* in *RPS4*-triggered but not in *RPM1*-triggered responses) and Group III genes (that require both *EDS1* and *PAD4* for maximal expression in untreated tissues) are shown in Supplemental Tables 2 and 3 online.

FMO1 Contributes to *EDS1* Defense

Upregulation of five of the genes in Group I and their dependence on *EDS1* and *PAD4* in *RPM1*-triggered resistance was verified by semiquantitative or quantitative RT-PCR analysis of total RNA in

Table 2. Group I Candidate Genes Induced by Pst *avrRpm1* in an *EDS1*- and *PAD4*-Dependent Manner

Probe Set ID ^a	AGI Number ^b	Gene Description	Gene Symbol
257185_at	At3g13100	ABC transporter	
260179_at	At1g70690	Kinase-related	
248062_at ^c	At5g55450	Lipid transfer protein	
256012_at	At1g19250	Flavin-containing monooxygenase	<i>FMO1</i>
263852_at	At2g04450	MutT/Nudix family	<i>NUDT6</i>
249743_at	At5g24550/At5g24540	Glycosyl hydrolase	
252060_at	At3g52430	Phytoalexin-deficient 4 protein	<i>PAD4</i>

^aProbe sets met the following criteria. (1) A \log_2 expression ratio of ≥ 1 upon *avrRpm1* versus MgCl_2 (at 3 and 6 h) in the wild type. (2) Suppression in both *eds1* and *pad4* versus the wild type ($\leq \log_2 -1$) at 3 and 6 h. Group I genes were also *EDS1/PAD4* dependent in *RPS4*-triggered resistance, but expression values at 3 h were below the threshold to meet selection criteria for Group II. (3) A P value ≤ 0.05 calculated by Wilcoxon rank sum test in MAS5.0. (4) An adjusted P value ≤ 0.05 using false discovery rate (FDR) adjustment (see Methods).

^bAGI, Arabidopsis Genome Initiative.

^c248062_at displayed a consistent *EDS1/PAD4* dependency and was therefore included in Group I but did not meet the criteria $\log_2 \geq 1$ in the ratio wild-type *avrRpm1*/wild-type MgCl_2 at 6 h as the absolute expression level in wild-type MgCl_2 at 6 h was already high.

two independent experiments (Figure 1). We investigated whether any of the Group I genes are necessary for plant *R* gene conditioned resistance by isolating corresponding T-DNA insertion mutants in *Arabidopsis* accession Columbia-0 (Col-0) and performing pathology assays (see Methods for a list of insertion lines). In all cases except one (*NUDT6*), we identified insertion lines with an interruption of the open reading frame (Figures 2A and 2B; see Supplemental Figure 1A online). Lines homozygous for each T-DNA insertion were inoculated with an isolate of the oomycete pathogen *Hyaloperonospora parasitica* (Cala2) that is recognized by the *TIR-NB-LRR*-type *R* gene *RPP2*. A T-DNA insertion in *FMO1* (denoted *fmo1-1*, Figure 2A) encoding a predicted flavin-dependent monooxygenase partially disabled *RPP2* resistance (Figure 2C). All other mutants produced discrete HR lesions at pathogen infection sites as seen in wild-type leaves (Figure 2C; see Supplemental Figure 1B online). Loss of resistance in *fmo1-1* was manifested as trailing plant cell necrosis that was more severe than in inoculated leaves of *sid2-1* (a mutant with a defect in the SA-biosynthetic enzyme isochorismate synthase; Wildermuth et al., 2001) but not as extreme as in *pad4-1* (Figure 2C). An independent Dissociation (Ds) insertion mutant of *FMO1* isolated in *Arabidopsis* accession Landsberg *erecta* (Ler-0) (denoted *fmo1-2*, Figure 2A) exhibited partial loss of resistance conditioned by the Ler-0 *TIR-NB-LRR* gene *RPP5* (recognizing *H. parasitica* isolate Noco2) similar to that of the Ler-0 *pad4* null mutant *pad4-2* (Figure 2D).

Pathology assays with Pst DC3000 strains expressing *avrRPS4* or *avrRpm1* established that the *fmo1-1* and *fmo1-2* mutations compromised *RPS4* but did not affect *RPM1* resistance, as shown for *fmo1-1* (Figure 3A). The Ler-0 *CC-NB-LRR* gene *RPP8* also conferred resistance to *H. parasitica* independently of *FMO1* (see Supplemental Figure 2 online). Basal resistance in *fmo1-1* (data not shown) and *fmo1-2* (Figure 3B) to virulent isolates of *H. parasitica* was reduced. These data show that defects in *FMO1* partially disable *TIR-NB-LRR* resistance and basal defense but can be overridden by *CC-NB-LRR* recognition. We concluded that *FMO1* specifically affects the *EDS1* pathway rather than promoting R protein-triggered resistance in general.

Defects in *Arabidopsis fmo1* Mutants Are Not Coupled to SA Accumulation

We assessed whether the *fmo1* mutant defects are associated with SA production. Levels of total SA were measured at 24 h in wild-type, *pad4-1*, and *fmo1-1* leaves after infiltration of Pst DC3000 expressing either *avrRpm1* or *avrRps4*. Leaves of *sid2-1* plants were infiltrated alongside as an SA-deficient control. *pad4-1* plants accumulated amounts of SA that were slightly reduced compared with the wild type after activation of *RPM1* resistance and were strongly reduced in *RPS4*-triggered tissues (Figure 4A). SA accumulation in *fmo1-1* was not significantly different from that of the wild type in *RPM1* and *RPS4* responses (Figure 4A). We concluded that *FMO1* is not essential for local SA production in either the CC- or *TIR-NB-LRR*-triggered resistance. To test further the hypothesis that *FMO1* activity is independent of SA, the *fmo1-1* mutation in Col-0 was crossed with *sid2-1* and homozygous double mutant lines selected. Single and double mutant combinations were then inoculated with *H. parasitica* isolate Cala2 (recognized by *RPP2*). The *fmo1-1 sid2-1* double mutant displayed loss of resistance that was significantly greater than either *sid2-1* or *fmo1-1* alone, measured by an increase in the frequency of trailing necrosis (Figure 4B) and pathogen spore production (Figure 4C). Therefore, the defects of *fmo1-1* and *sid2-1* in *TIR-NB-LRR* resistance are genetically additive and consistent with incremental activities of *FMO1* and *SID2* in defense signal relay. These data argue for a role of *FMO1* in an SA-independent branch of the *EDS1* pathway that, together with SA production, is required for full expression of resistance.

FMOs bind the cofactor flavin adenine nucleotide (FAD) and catalyze oxygenation of substrates containing nucleophilic nitrogen, phosphorous, sulfur, or selenium at the expense of NADPH. Extensively studied mammalian *FMOs* function in detoxification of xenobiotics (Lawton et al., 1994); the single yeast *FMO* (*yFMO*) acts as a redox regulator by oxidizing biological thiols (Suh et al., 1999), and an insect *FMO* (*SNO*) inactivates a plant toxin (Naumann et al., 2002). Little is known about *FMO* proteins in plants. One *FMO* clade containing *Arabidopsis Yucca* homologs and the *Floozy* gene from *Petunia* was shown to *N*-hydroxylate

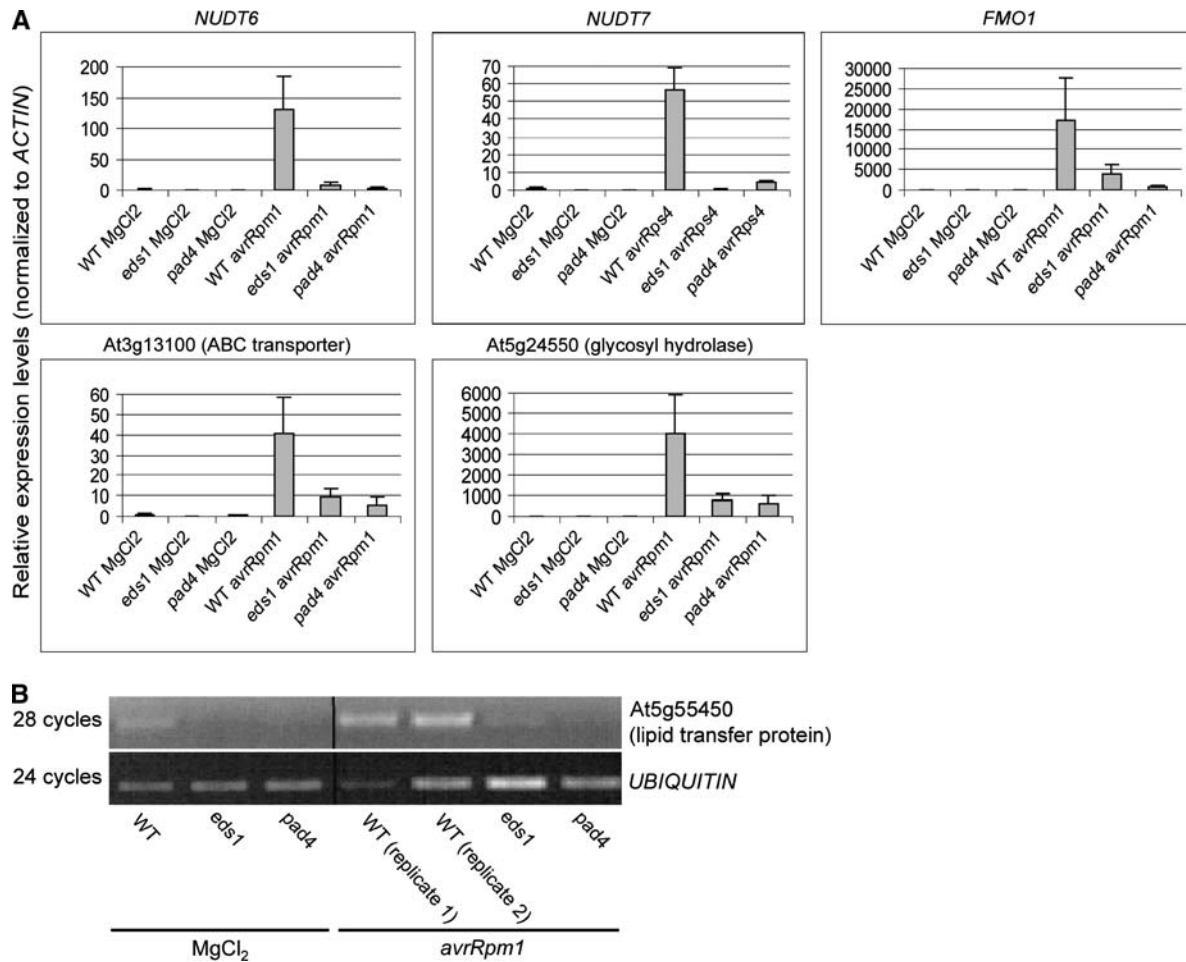


Figure 1. RT-PCR Analysis for Group I Genes and *NUDT7* in Wild-Type and Mutant Plants.

(A) Relative transcript levels were determined by quantitative real-time PCR as described in Methods. Expression levels were normalized with respect to the internal control *ACTIN* and displayed relative to the expression in mock-treated wild-type samples (WT MgCl₂, with a relative expression value set at 1). Data bars represent the mean levels of transcripts (\pm SD, $n = 3$).

(B) Semiquantitative RT-PCR analysis for At5g55450. *UBIQUITIN* expression was used to standardize transcript levels in each sample. A second RT-PCR experiment with independent RNA samples gave similar results.

tryptamine in a proposed step of auxin biosynthesis (Zhao et al., 2001; Tobena-Santamaria et al., 2002). Sequencing of *FMO1* cDNA derived from Col-0 revealed that the published The Arabidopsis Information Resource (TAIR) coding sequence (CDS) for At1g19250 lacks a stretch of 45 nucleotides in exon 4 (<http://www.arabidopsis.org/>). The coding sequence (1593 bp) was translated to a 530-amino acid sequence that is identical to protein AAF82235 from the National Center for Biotechnology Information database (<http://www.ncbi.nlm.nih.gov/>), and this was used in further analyses. Multiple sequence alignments of *FMO1* with functionally characterized FMOs from *Arabidopsis*, bacteria, yeast, insect, and humans showed that *FMO1* possesses an FAD binding site, an FMO-identifying motif, and an NADPH binding domain that are characteristic of functional FMO enzymes (Figure 5A). Lack of conservation of the second Gly of the NADPH binding domain in *FMO1* occurs also in a catalytically functional bacterial FMO (Figure 5A; Choi et al., 2003). Previous

phylogenetic analyses show that *Arabidopsis* FMO-like proteins form three distinct clusters (Fraaije et al., 2002; Naumann et al., 2002). *FMO1* and another gene, At5g45180, are the sole representatives of one of the three clusters. Microarray data from this study and from the Affymetrix database of the Nottingham Arabidopsis Stock Centre (NASC; <http://arabidopsis.info/>) reveal that At5g45180 (ATH1 array element 248987_at) is not expressed and therefore likely to be a pseudogene. A BLASTP database search identified an FMO-like protein in rice (*Oryza sativa*) of unknown function with 56% amino acid identity (Os FMO, Figure 5A).

Other analyses have demonstrated the importance of the conserved Gly residues in the FAD and NADPH binding sites for cofactor binding and enzymatic activity (Rescigno and Perham, 1994; Kubo et al., 1997). We therefore generated by site-directed mutagenesis variants of *FMO1* in which the conserved Gly residues of these motifs were exchanged to Ala residues (Figure 5A).

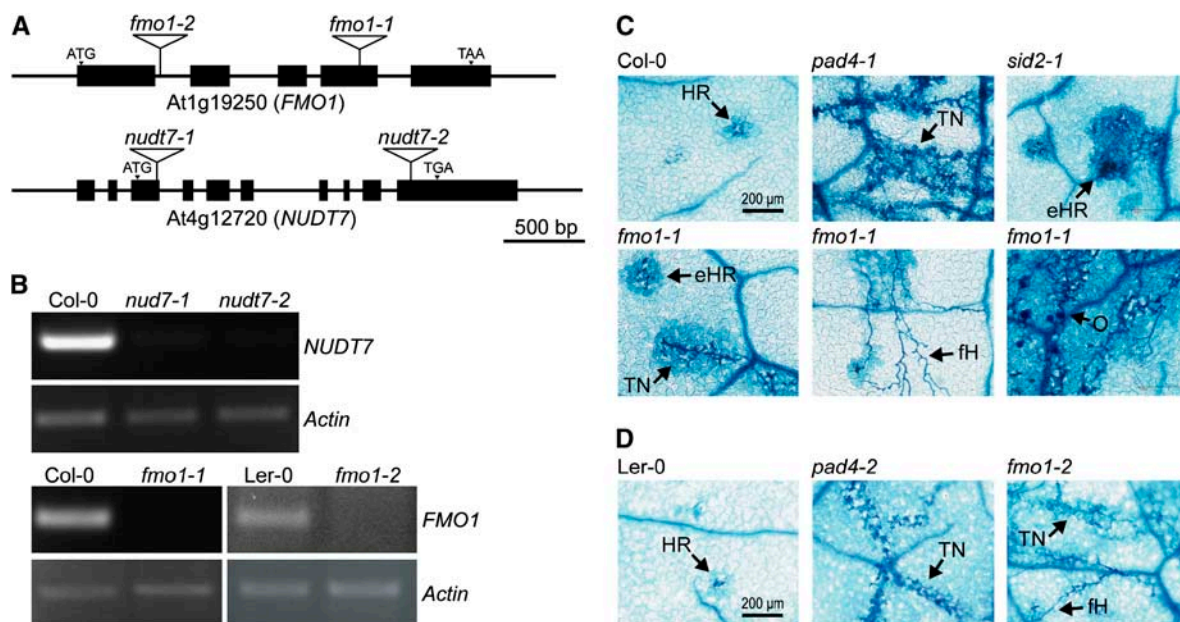


Figure 2. Defects in *FMO1* Compromise TIR-NB-LRR-Triggered Resistance.

(A) Schematic representation of *FMO1* and *NUDT7* genomic structures with exons represented as black boxes. The positions of T-DNA and Ds insertions (*fmo1-2*) are indicated.

(B) RT-PCR of RNA isolated from leaves of the indicate plant genotypes. *ACTIN* mRNA was used to normalize transcript levels in each sample (see Methods).

(C) Resistance to *H. parasitica* isolate Cala2 conferred by the *TIR-NB-LRR*-type *R* gene *RPP2* in Col-0 wild-type and defense mutant lines. Lactophenol trypan blue-stained leaves were viewed under a light microscope for pathogen structures and plant cell death 6 d after inoculation. HR, tightly delimited plant cell death; eHR, extended HR; TN, trailing necrosis; fH, free pathogen hyphae; O, oospores. Images are representative of at least 18 plants per genotype. Similar results were obtained in two independent experiments.

(D) Response phenotypes of the wild type (Ler-0), *pad4-2*, and *fmo1-2* to avirulent *H. parasitica* isolate Noco2 (recognized by *RPP5*). Inoculation and staining procedures were as described in **(C)**.

Wild-type *FMO1* and the *fmo1* mutants under the control of the cauliflower mosaic virus 35S promoter and fused to a C-terminal StreptII affinity purification tag were stably transformed into *fmo1-1*, and several independent single insertion homozygous lines were selected for each construct. Although constitutively expressed wild-type *FMO1* protein was hardly detectable in transgenic leaf extracts (Figure 5B), it complemented the *fmo1-1* defect in basal resistance to virulent *H. parasitica* (Figure 5C). Moreover, constitutive expression of *FMO1* caused significantly enhanced resistance in two out of three independent transgenic lines (Figure 5C). By contrast, accumulation of the predicted catalytically inactive *fmo1* variant proteins was much higher than wild-type *FMO1* (Figure 5B), but these failed to complement the *fmo1-1* defect in basal resistance (Figure 5C). We concluded that intact FAD and NADPH binding are required for *FMO1* defense function.

Mutations in *NUDT7* Encoding a Cytosolic Nudix Hydrolase Deregulate Resistance

Expression of *NUDT6* (At2g04450), encoding a putative cytosolic Nudix hydrolase, was also strongly *EDS1* and *PAD4* dependent after triggering of *RPM1* resistance (Table 2). However, a loss-of-function mutant of this gene was not found. A T-DNA insertion

was identified in the promoter of *NUDT6*, but this did not deplete its mRNA (see Supplemental Figure 1 online). We noted that a second predicted cytosolic Nudix hydrolase, *NUDT7* (At4g12720), that is highly sequence related to *NUDT6* (61% amino acid identity; Figure 6) was also strongly induced in *RPM1* and *RPS4* responses and was registered as *EDS1* and *PAD4* dependent in the *RPS4*-triggered tissues using our selection criteria (see Supplemental Table 2 online). In another study, *NUDT7* was identified among seven *PAD4* coregulated genes (including *EDS1*) in SA-independent resistance conditioned by *RPP4* (a *TIR-NB-LRR*-type gene) (Eulgem et al., 2004). Nudix (for nucleoside diphosphates linked to moiety X) hydrolases that are characterized by a conserved motif, $GX_5EX_7REVXEEEXGU$ (where U is Ile, Leu, or Val), are found in a wide range of species from viruses to humans (McLennan, 1999). They catalyze hydrolysis of nucleoside diphosphate derivatives and have been shown to regulate levels of toxic molecules and signal intermediates in the cell (Bessman et al., 1996; Perraud et al., 2005).

Disruption of *NUDT7* in two independent T-DNA insertion lines, denoted *nudt7-1* and *nudt7-2* (Figures 2A and 2B), caused visible growth retardation (Figures 7A and 7B) and strongly enhanced basal resistance to virulent *H. parasitica* (Figure 7C) suggestive of deregulated defense in these mutants. Consistent with a constitutive resistance phenotype, SA levels were approximately

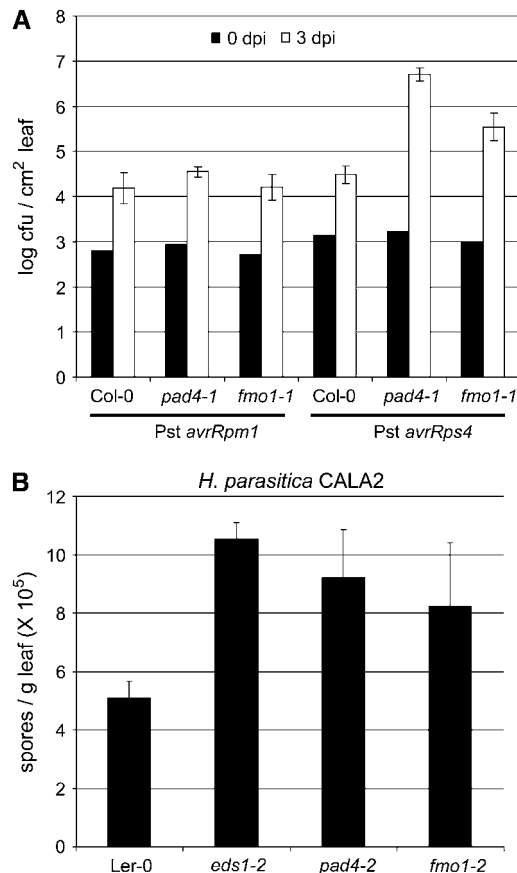


Figure 3. Pathogen Growth in *Arabidopsis fmo1* Mutants.

(A) *RPM1* (CC-NB-LRR) resistance to *Pst avrRpm1* is not compromised in *fmo1-1*, whereas *RPS4* (TIR-NB-LRR) resistance to *Pst avrRps4* is reduced. Leaves of 5-week-old plants were vacuum infiltrated with bacterial suspensions at 5×10^5 cfu/mL and bacterial titers determined in triplicate at 0 and 3 d after inoculation (dpi). Data points are the average of three replicate samples (\pm SD).

(B) Basal resistance of Ler-0 leaves to virulent *H. parasitica* isolate Cala2 is reduced in *fmo1-2*. Numbers of pathogen conidiospores were measured on leaves 6 d after inoculation. Values are the average of four replicate samples (\pm SD).

fourfold higher in *nudt7-1* compared with the wild type (Figure 7D). In pathogen assays, we observed an increase in the number of dead cells in *nudt7* leaves in response to avirulent *H. parasitica*. This prompted us to examine *nudt7* mutants for appearance of necrotic lesions in pathogen-unchallenged plants under normal growth conditions in soil. The *nudt7* mutants exhibited spontaneous death of individual cells in leaves of 2-, 3-, and 4-week-old (Figure 7E) plants viewed under the microscope after staining for dead cells with lactophenol trypan blue.

Multiple *Arabidopsis* mutants have been identified that deregulate plant cell death (Lorrain et al., 2003). Some of these mutants, such as *acd11* (Brodersen et al., 2002) and *lsd1* (Rustérucchi et al., 2001), depend on the *EDS1* pathway to transduce signals leading to cell death. We tested whether the developmental defects and enhanced basal resistance in *nudt7*

require functional *EDS1* by combining *nudt7-1* with the null *eds1-2* mutation (Feys et al., 2001) that had been introgressed into Col-0 (Col *eds1-2*). Growth retardation (Figures 7A and 7B), enhanced resistance to virulent *H. parasitica* (Figure 7C), and lesioning (Figure 7E) in *nudt7-1* were abolished in the presence of *eds1-2*. We concluded that signals in *nudt7-1* leading to deregulated disease resistance and cell death are channeled entirely through *EDS1*. *nudt7-1* was also combined with *sid2-1* to assess whether SA accumulation is necessary for the deregulated resistance phenotype. Surprisingly, *nudt7-1 sid2-1* mutants were even more retarded in growth (Figures 7A and 7B) and displayed a higher frequency of spontaneous cell death (Figure 7F) compared with the *nudt7* single mutants. Basal resistance of *nudt7-1 sid2-1* mutants was intermediate between that exhibited by *sid2-1* and *nudt7-1*. We confirmed that the marked difference in phenotypes between *nudt7-1 eds1-2* and *nudt7-1 sid2-1* plants was not attributable to differences in SA accumulation since both lines were strongly depleted in total SA (Figure 7D). These data show that growth retardation and cell death initiation in *nudt7-1* require *EDS1* but are antagonized by SA. By contrast, both SA-dependent and SA-unrelated processes contribute to enhanced resistance of *nudt7* mutants to *H. parasitica*.

DISCUSSION

EDS1 regulatory complexes are needed for expression of plant basal resistance against invasive pathogens and connect specific pathogen recognition by TIR-NB-LRR-type immune receptors to activation of basal defenses (Feys et al., 2005; Lipka et al., 2005). Here, we used *Arabidopsis* gene expression microarrays to identify potential new components of the *Arabidopsis* *EDS1* pathway. Phenotypic analysis of insertion mutants in a discrete set of *RPM1*-induced *EDS1/PAD4*-regulated *Arabidopsis* genes (Group I; Table 2) uncovered one positive regulator of *EDS1* signaling, *FMO1*. By cross-referencing Group I and Group II (*RPS4*-induced *EDS1/PAD4*-regulated; see Supplemental Table 2 online) genes, we discovered one member of a family of cytosolic Nudix hydrolases (*NUDT7*) that negatively regulates *EDS1*-conditioned plant defense and programmed cell death. Insertion mutants corresponding to the remaining Group I genes did not display altered defense in *RPP2* or basal resistance (see Supplemental Figure 1 online). It is possible that functional redundancy might have hindered identification of an altered defense phenotype. For example, the *lipid transfer protein-like* gene At5g55450 has three sequence-related genes. Two of these (At5g55410 and At5g55460 lying in tandem on *Arabidopsis* chromosome 5) are pathogen inducible as measured by RT-PCR (M. Bartsch and J.E. Parker, unpublished data). The third gene, *DEFECTIVE IN INDUCED RESISTANCE1* (At5g48485), is not pathogen responsive but was shown to contribute to establishment of plant systemic resistance (Maldonado et al., 2002).

FMO1 is required for full expression of TIR-NB-LRR-conditioned resistance to avirulent pathogens and for basal resistance to invasive virulent pathogens (Figures 2 and 3). As in plants with defects in *EDS1* or its interacting partners *PAD4* and *SAG101* (Feys et al., 2005), the deficiency of an *fmo1-1* null mutant is overridden by *RPM1* and *RPP8* recognition. All of these features are consistent with a role of *FMO1* in the *EDS1* pathway.

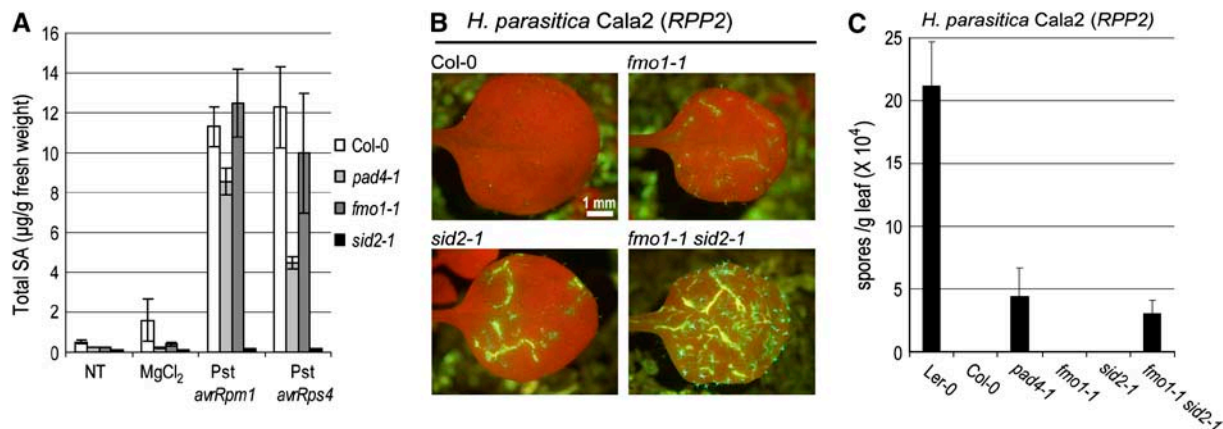


Figure 4. Attenuated Resistance in *Arabidopsis fmo1* Plants Is Uncoupled from Impaired SA Accumulation.

(A) Total SA levels were measured in leaves of 4-week-old plants that were either untreated (NT) or 24 h after vacuum infiltration with 10 mM MgCl₂, 5 × 10⁶ cfu/mL Pst *avrRpm1*, or Pst *avrRps4* in 10 mM MgCl₂. Data represent the average of three replicate samples (±SD).

(B) Response phenotypes of wild-type and mutant plants 5 d after inoculation of leaves with avirulent *H. parasitica* Cala2 (4 × 10⁵ spores/mL; recognized by RPP2) in Col-0). Leaves were viewed on a binocular microscope under UV light to visualize cell death-associated fluorescence indicative of plant trailing necrosis.

(C) Spore production on leaves of single and double mutant lines 6 d after inoculation with avirulent *H. parasitica* isolate Cala2 (recognized by RPP2 in Col-0 and virulent on Ler-0). Data points are the average of four replicate samples (±SD).

Uncoupling *fmo1-1* defects from SA accumulation (Figure 4) further supports a function of FMO1 in an EDS1-regulated but SA-independent mechanism that promotes resistance and cell death at pathogen infection sites.

EDS1 and PAD4 drive defense signal amplification involving positive feedback on expression of multiple genes, including themselves (Wiermer et al., 2005). We assessed whether *fmo1-1* affects PAD4 or EDS1 mRNA accumulation. We found that EDS1 and PAD4 transcripts were marginally reduced in *fmo1-1* compared with the wild type in healthy tissues and were not significantly affected in pathogen-treated tissues (M. Bartsch and J.E. Parker, unpublished data), inconsistent with a primary role of FMO1 in stimulating expression of these regulators. Instead, we favor the idea that FMO1 acts posttranslationally on one or more EDS1 pathway components. Like EDS1 and PAD4 (Feys et al., 2001), preexisting FMO1 protein inside the cell may exert a major activity once the plant defense pathway is triggered and together with other positive and negative components be subject to rapid upregulation, as demonstrated here. Pathology tests of *fmo1-1* stable transgenic lines constitutively expressing wild-type FMO1 showed that they were complemented for pathogen resistance, whereas transgenics expressing *fmo1* amino acid exchange variants in the conserved Gly residues of the FAD and NADPH binding motifs were not (Figure 5C). Thus, flavin-dependent monooxygenase activity is required for FMO1 defense function. The marked difference in accumulation of wild-type FMO1 and the catalytically inactive *fmo1* variants coupled with enhanced basal resistance only of *fmo1-1* plants expressing wild-type FMO1 suggests that active FMO1 strongly influences the degree of resistance. FMO1 levels may therefore be strictly regulated inside the cell. Uncovering the precise biochemical activity of FMO1 should provide insight into processes involved in EDS1 signaling. One possibility is that FMO1 regulates oxidative me-

tabolism, as was found for the single yeast FMO protein (Suh et al., 1999). Brodersen et al. (2002) reported that FMO1 (referred to as FMO) mRNA accumulates to high levels in the *acd11* mutant that triggers EDS1-dependent cell death. Recent studies reveal that FMO1 was also transcriptionally upregulated in response to superoxide generation but not by hydrogen peroxide or ozone (Olszak et al., 2006), suggesting a close link between provision of certain ROS and FMO1 expression. In the same study, FMO1 mRNA was elevated in the *lsd1* mutant but not in the constitutive defense mutants *ctr1*, *cec1*, *cpr6-1*, or *mpk4*, indicating that FMO1 is not activated simply by deregulating SA, jasmonic acid, or ethylene signaling (Olszak et al., 2006). An intrinsic activity of EDS1 and PAD4 is to process ROS-derived signals in biotic and abiotic stress responses (Rustérucchi et al., 2001; Mateo et al., 2004). FMO1 may alter the redox state of a signal intermediate or components of the EDS1 system to promote signal relay. Alternatively, FMO1 could N- or S-oxygenate a molecule that contributes additively with SA to resistance.

Our genetic analyses show that growth inhibition, enhanced basal resistance, and lesioning of *nudt7* plants also depend on functional EDS1 (Figure 7). Strikingly, the sporadic death of individual cells in the epidermis and palisade and spongy mesophyll layers of *nudt7* leaves (Figure 7E) did not progress to confluent lesioning, suggesting that NUDT7 normally restricts the initiation rather than propagation of cell death. Also, lesion formation in *nudt7* did not depend on isochorismate synthase encoded by SID2 (Figures 7E and 7F) that provides the major route for pathogen-induced SA accumulation (Wildermuth et al., 2001). Instead, SA depletion exacerbated *nudt7-1* conditioned cell death (Figures 7E and 7F) and growth retardation (Figures 7A and 7B). This contrasts markedly with deregulated cell death in *acd11* or *lsd1* that require functional SID2 (Brodersen et al., 2005; Torres et al., 2005). In *lsd1* leaves, SA appears to act as a

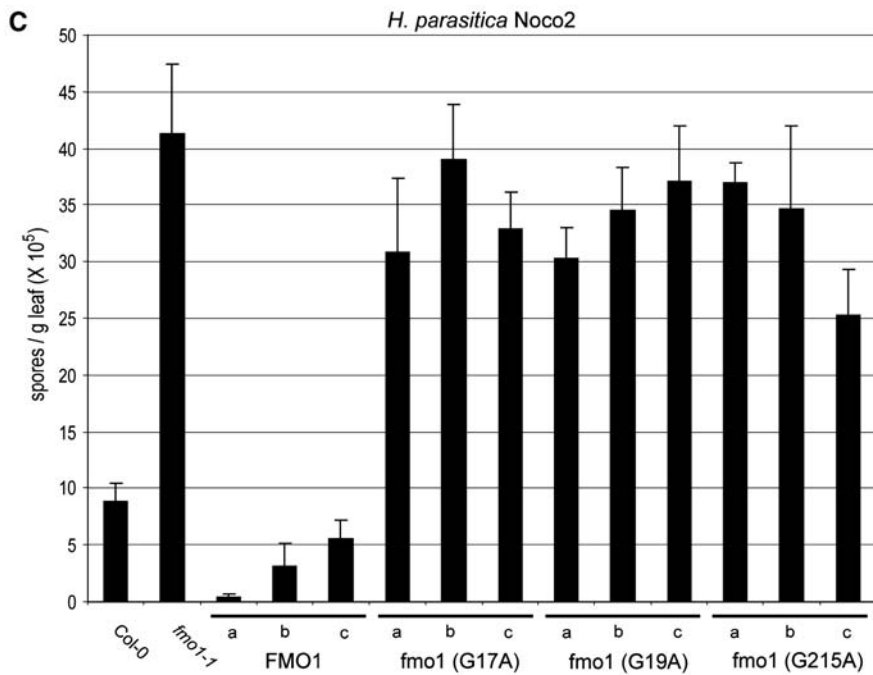
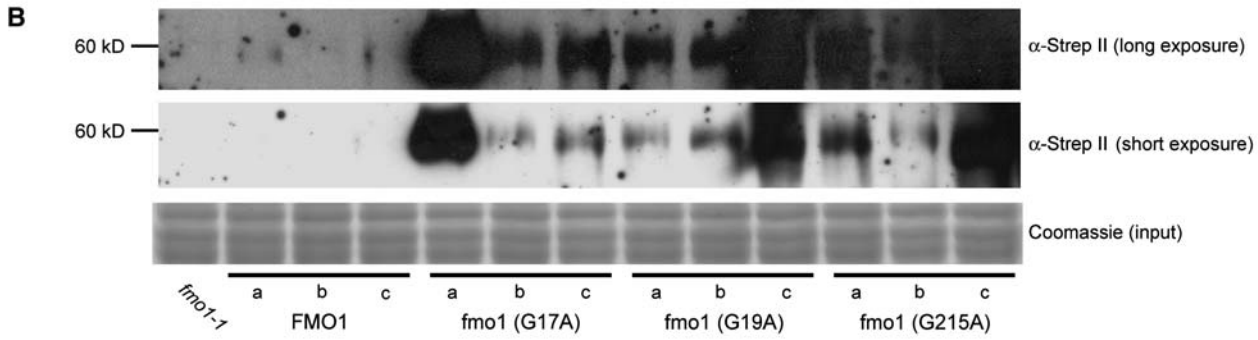
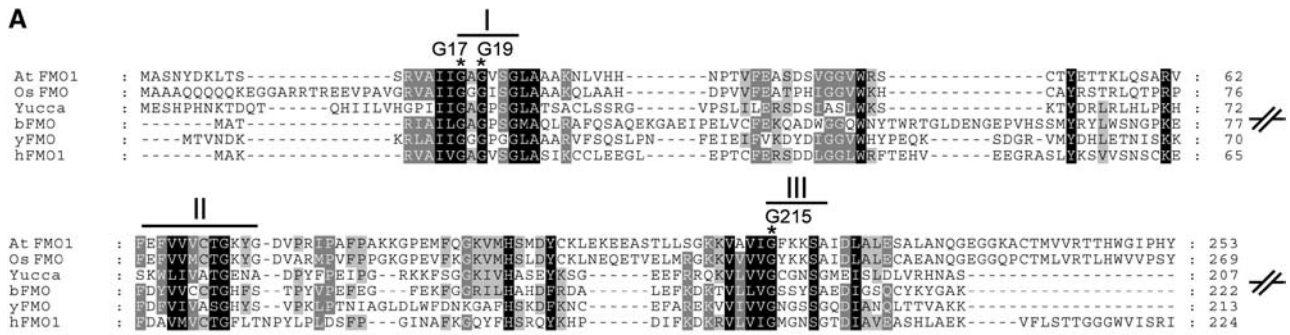


Figure 5. FMO1 Catalytic Domains Are Required for Defense Signaling.

(A) Alignment of amino acid sequences from *Arabidopsis* (At FMO1 and YUCCA; Zhao et al., 2001), rice (Os FMO), *Methylophaga* sp Strain SK1 (bFMO; Choi et al., 2003), yeast (yFMO; Zhang and Robertus, 2002), and human (hFMO1; Lawton et al., 1994) was performed, and the N-terminal sequences are shown here. FMO-defining motifs and the conserved Gly residues exchanged by site-directed mutagenesis are indicated above the top line: I, FAD binding motif GXGXXG; II, FMO identifying sequence motif FXGXXXHXXX(Y/F); and III, NADPH binding domain GXGXX(G/A). Multiple alignments were visualized using GeneDoc (Nicholas et al., 1997) with conserved residue shading mode set to level 4 using default settings and enabled similarity groups function. Amino acids with 100, 80, and 60% conservation are presented as white letters on black background, white letters on dark-gray background, and black letters on light-gray background, respectively.

(B) Expression of wild-type and mutant forms of FMO1-StrepII in independent *fmo1-1* transformants. Protein gel blot analysis was performed after StrepII affinity purification. Equal amounts of the input fraction are shown by Coomassie blue staining.

(C) Intact FAD and NADPH binding sites in FMO1 are required for basal resistance to virulent strain *H. parasitica*. The plant lines correspond to those tested in **(B)**. Numbers of pathogen conidiospores were measured on leaves 6 d after inoculation. Values are the average of four replicate samples (±SD).

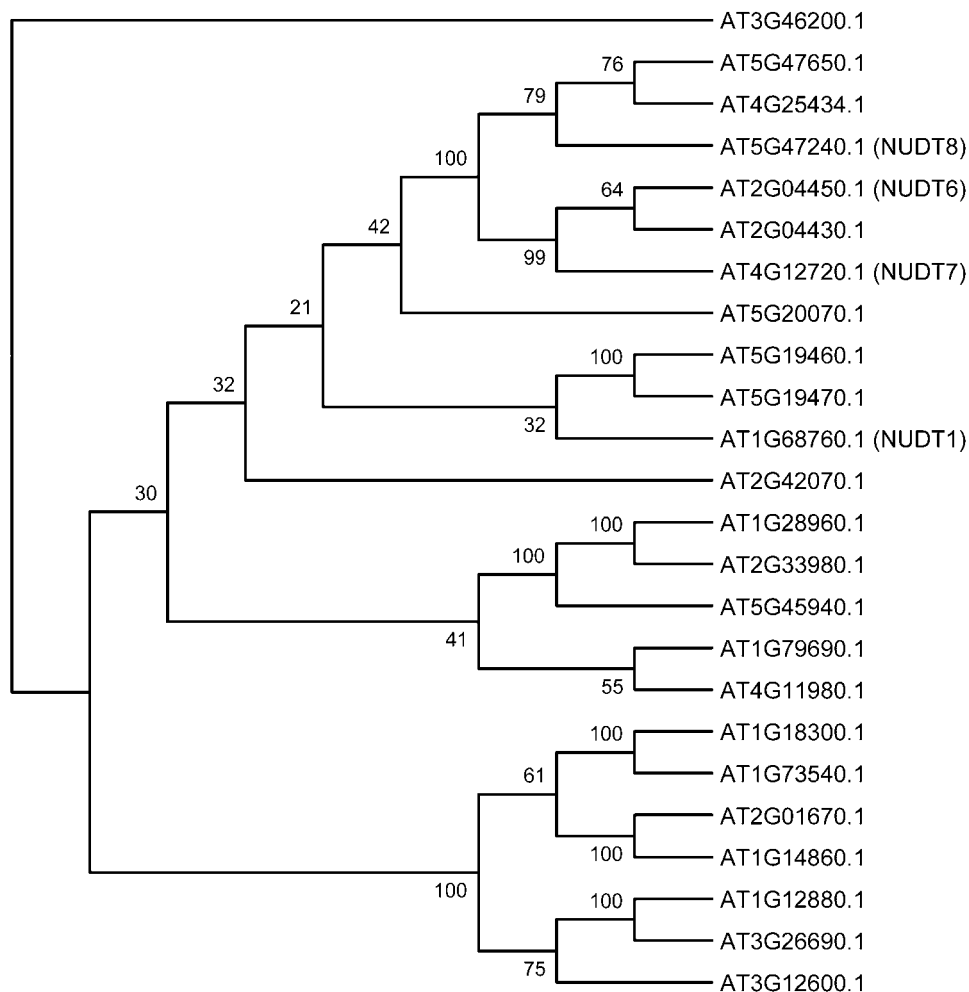


Figure 6. Phylogeny of *Arabidopsis* Nudix Hydrolase Family Members.

A phylogenetic tree drawn from neighbor-joining analysis using Mega 3.0 software (Kumar et al., 2004). Bootstrap values (1000 replicates) are shown. Annotations of Nudix hydrolase-like proteins were taken from Ogawa et al. (2005).

promotive signal in propagation of cell death that is inhibited by NADPH-oxidase generated ROS (Torres et al., 2005). These and our data imply differences in signal relay between cell death initiation and maintenance programs. Although *sid2-2* mutants suppressed *acd11*-triggered cell death and SA accumulation, application of SA to *acd11 sid2-2* leaves failed to restore lesioning indicative of isochorismate synthase-derived compounds other than SA as mediators of programmed cell death in *acd11* (Brodersen et al., 2005). While aspects of *acd11* and *nudt7* phenotypes are clearly distinct, both deregulated resistance pathways generate *EDS1*-dependent signals that are not SA itself. Recent studies showed that NUDT6 and NUDT7 hydrolyze preferentially ADP-ribose and NADH in vitro (Ogawa et al., 2005; Olejnik and Kraszewska, 2005). In mammalian cells, ADP-ribose has been implicated as an intracellular second messenger in oxidative stress-induced ion channel activation and apoptosis (Perraud et al., 2001, 2005; Kolisek et al., 2005). Levels of free ADP-ribose increase under oxidative stress conditions due to NAD^+ decay catalyzed by the enzymes

PARP/PARG (poly-ADP-ribose polymerase/poly-ADP-ribose glycohydrolase) in the nucleus or by mitochondrial damage and subsequent ADP-ribose leakage (Richter and Schlegel, 1993; Kolisek et al., 2005). A role for free ADP-ribose in plant cells is unknown but as a potentially toxic intermediate that can modify and inactivate proteins by mono-ADP-ribosylation (McDonald et al., 1992; Bektas et al., 2005), and its levels are likely to be strictly controlled. Downregulation of PARP enzymes that could potentially produce ADP-ribose rendered plants more tolerant to a broad range of stresses (De Block et al., 2005). A requirement for *EDS1* and *PAD4* in pathogen-stimulated accumulation of NUDT6 and NUDT7 enzymes that would eliminate ADP-ribose suggests that ADP-ribose might be generated through *EDS1/PAD4* activity as a proapoptotic and resistance promoting signal. Therefore, these Nudix hydrolases could serve to restrict the damaging effects of the plant defense response. Supporting this idea, several pathogen-derived Nudix enzymes were shown to contribute to infectivity of mammalian cells and may protect the pathogen against damaging oxidative stresses

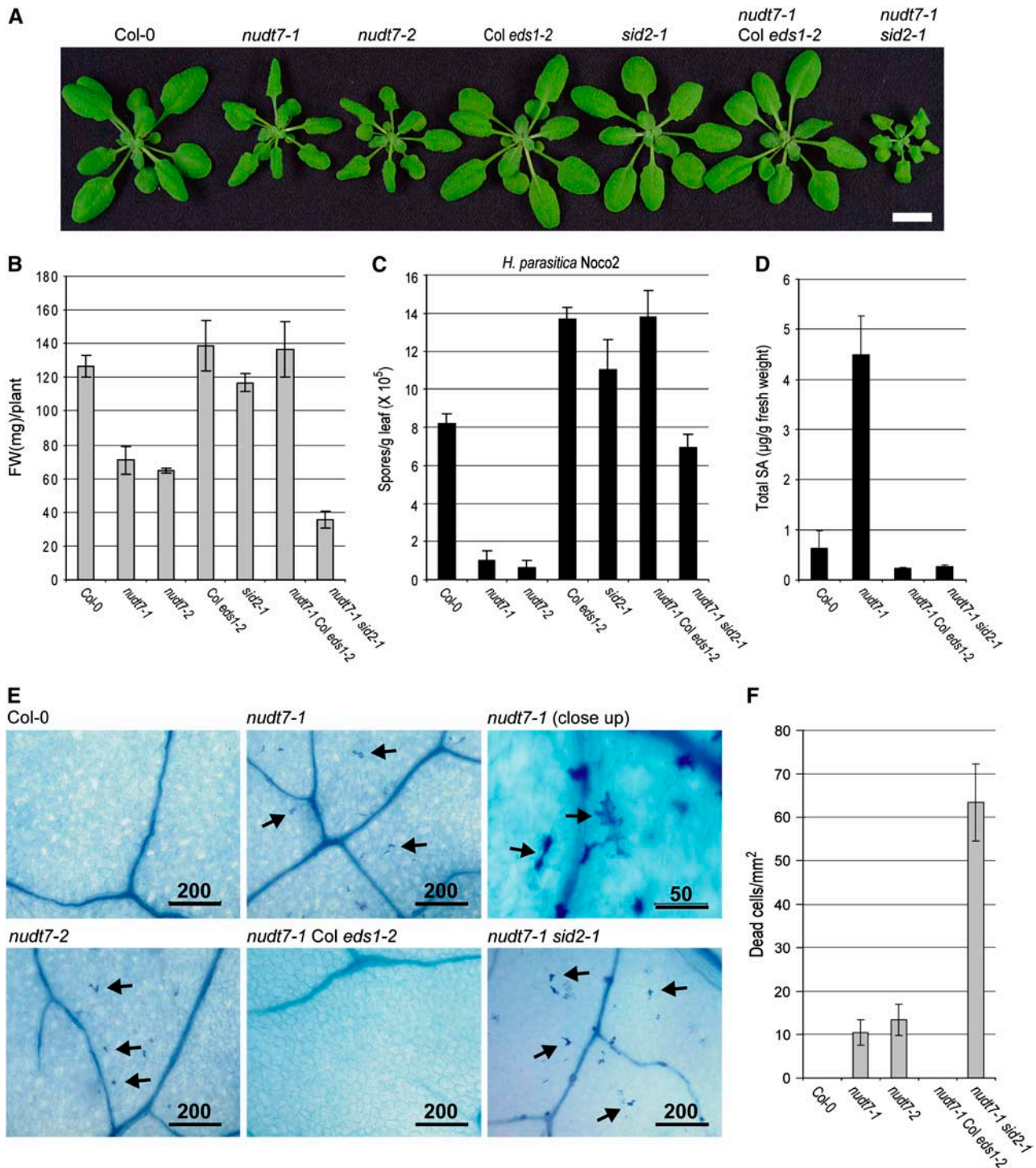


Figure 7. Developmental and Basal Resistance Phenotypes of *nudt7* Single and Double Mutants.

(A) Attenuated growth of *nudt7-1* is suppressed by *eds1-2* but exacerbated by *sid2-1*. Four-week-old soil-grown plants representative of single or double mutants are shown. Bar = 1 cm.

(B) Average fresh weight (FW) of 4-week-old plants (\pm SD) calculated from the aerial tissue weight of six plants per genotype.

(C) Enhanced basal resistance to *H. parasitica* isolate Noco2 in *nudt7* mutants is dependent on *EDS1* and partially requires *SID2*. Pathogen spores were counted as in Figure 3B.

(D) Levels of total SA in leaves of healthy 4-week-old plants. Data points are the average of three replicate samples (\pm SD).

(E) Visualization of dead cells in leaves of 4-week-old *nudt7* single and double mutants after staining with lactophenol trypan blue. The scale bar unit is in micrometers.

(F) Quantification of leaf cell death. Numbers of dead cells were determined in leaves of 3-week-old plants after staining with lactophenol trypan blue. Data represent samplings from 10 leaves from at least five plants per genotype (\pm SD). Single cell death did not occur in *Col eds1-2* or *sid2-1* (data not shown).

at infection sites (McLennan, 1999; Kang et al., 2003). Moreover, *NUDT6* and *NUDT7* were listed as upregulated genes in a microarray analysis of *Arabidopsis* mutants lacking a functional cytosolic ascorbate peroxidase (APX1), a key enzyme of H₂O₂ removal in plants under light stress (Davletova et al., 2005).

Elucidating the precise in vivo activities of FMO1 and Nudix hydrolase enzymes should help to define key steps of the EDS1 pathway. It may also clarify the complex relationship between SA, ROS signals, and cell death in plant immune responses.

METHODS

Plant Material and Mutant Characterization

Arabidopsis thaliana wild-type Ws-0, Ler-0, Col-0, *eds1-1* (Falk et al., 1999), *pad4-5*, *pad4-1* (Jirage et al., 1999), and *sid2-1* (Wildermuth et al., 2001) mutants have been described. The null *eds1-2* mutation in the Col-0 background (referred to as Col *eds1-2*) was derived from a cross between Col-0 and *eds1-2* (Ler-0) followed by eight backcrosses to Col-0. Insertion mutants of *EDS1/PAD4*-dependent genes were identified using the SIGnAL T-DNA Express *Arabidopsis* gene mapping tool (<http://signal.salk.edu/>). SALK lines SALK_026163 (*fmo1-1*), SALK_046441 (*nudt7-1*), and SALK_104293 (*nudt7-2*) and Ds insertion line (Sundaresan et al., 1995) GT_3_108523 (*fmo1-2*) were distributed by the NASC (<http://arabidopsis.info/>). Homozygous insertion mutants were identified by PCR using T-DNA- and gene-specific primer sets as described on the T-DNA Express homepage. Primer sequences are available on request. To evaluate if the isolated mutants were mRNA nulls, semiquantitative RT-PCR was performed using gene-specific primers: *FMO1*-forward (5'-GGAAGCGGATAAAGGGATGATCC-3'), *FMO1*-reverse (5'-TTAAGCAGTCATATCTCTTTTCTTC-3'), *NUDT7*-forward (5'-TTGTAGGTGCTGGTGCTTTG-3'), *NUDT7*-reverse (5'-GCGATACTTTAAGGCGCTTG-3'), *ACTIN*-forward (5'-TGCGACAATGGAAGTGAATG-3'), and *ACTIN*-reverse (5'-CTGTCTCGAGTTCCTGCTCG-3'). Double mutants were generated by crossing individual mutants and identifying homozygous double mutant combinations by PCR or sequencing of PCR-amplified DNA fragments. T-DNA insertion lines of genes in Group I that exhibited no defects in *RPP2* resistance are SALK_120950 (At3g13100), SAIL_46_E06 (At1g70690), SALK_109557 (At5g55450), and SALK_038957 (At5g24540).

Plant Growth and Pathology Assays

Plants were soil grown in controlled environment chambers under a regime of a 10-h light period at 150 to 200 $\mu\text{E m}^{-2} \text{s}^{-1}$, 23°C, and 65% relative humidity. Four-week-old plants were used for microarray experiments, 2-week-old plants for infection assays with *Hyaloperonospora parasitica*, and 4- to 5-week-old plants for infections with *Pseudomonas syringae* strains. *H. parasitica* was spray inoculated at 4×10^4 unless otherwise stated. Detailed procedures for pathogen inoculations and determination of pathogen growth have been described (Feys et al., 2005). *P. syringae* inoculations of leaves were done with a needleless syringe for microarray sampling or by vacuum infiltration for bacterial growth assays. Plant cell death and *H. parasitica* infection structures were visualized under a light microscope after staining of leaves with lactophenol trypan blue (Aarts et al., 1998).

Microarray Sampling and Data Collection

Leaves were harvested at the indicated time points (Table 1) and total RNA extracted using RNAwiz reagent (Ambion). cRNA was prepared following the manufacturer's instructions (www.affymetrix.com/support/technical/manual/expression_manual.affx). Labeled cRNA transcripts

were purified using the Sample Cleanup Module (Affymetrix). Fragmentation of cRNA transcripts, hybridization, and scanning of the high-density oligonucleotide microarrays (*Arabidopsis* ATH1 genome array; Affymetrix) were performed according to the manufacturer's GeneChip Expression Analysis Technical Manual.

Microarray Data Analysis

For data collection and assessment, we used Affymetrix Microarray Analysis Suite Version 5.0 (MAS5.0) and R language (bioconductor project). Following standard protocols for data analysis using MAS5.0, the fluorescence intensity of each array was scaled to an overall intensity of 100 to enable comparison of all arrays. Signal log ratios and corresponding P values were calculated using standard MAS5.0 algorithms (statistical algorithms description document, technical report; Affymetrix, 2002). As a second approach for background adjustment, normalization, and collation, we used the RMA (robust multichip average) model in R language (Irizarry et al., 2003). Fold changes were calculated based on signal values derived by the RMA method. To assign a level of confidence for expression differences between the different experimental conditions, P values were calculated for each probe set individually by conducting a paired Wilcoxon rank sum test based on 11 individual values (mismatch signal subtracted from the perfect match signal) of a respective probe set. FDR calculations were performed according to the Benjamini and Hochberg definition of FDR (Benjamini and Hochberg, 1995) in R language (multitest package). Hierarchical cluster analysis was performed in R language (hclust package). Annotations of *Arabidopsis* genes based on the probe set identifiers were obtained from TAIR (www.arabidopsis.org).

RT-PCR Analysis

Total RNA was extracted as described for the preparation of the microarray samples. RT reactions were performed with 1 μg of total RNA and 0.5 μg of oligo(dT)₁₈ primer at 42°C using reverse transcriptase and RNAase inhibitor RNasin (both from Promega) in a 20- μL reaction volume. Aliquots of 1 μL RT-reaction product were subsequently used for quantitative and semiquantitative RT-PCR analysis using the following gene-specific primers: *NUDT6*-forward (5'-CACCATGGACAATGAAGATCAGGAGTC-3'), *NUDT6*-reverse (5'-TCAACCAGAGGTGGAGGCTAG-3'), At3g13100-forward (5'-GGCACTCTCTTTTTCAGTGTGGC-3'), At3g13100-reverse (5'-GGAACCTTCATCTCCATCCTTGAA-3'), At524550-forward (5'-CGTACCGGCGACACCATCTCA-3'), At524550-reverse (5'-TTAAATCATCTGTAATGTAGACCAC-3'), At5g55450-forward (5'-GACAACAC-CAGAATCCTCATGCAA-3'), At5g55450-reverse (5'-GTAGTACACAATG-GAGTTAGCAA-3'), *UBIQUITIN*-forward (5'-AACTTTCTCTCAATCTCTCTACC-3'), and *UBIQUITIN*-reverse (5'-CCACGGAGCCTGAGGACCAAGTGG-3'). Primers for *ACTIN*, *FMO1*, and *NUDT7* were as described for the mutant characterization. RT-PCR conditions were as follows: 95°C for 10 min and 50 cycles of 95°C for 30 s, 55°C for 30 s, and 72°C for 1 min and 30 s. Relative transcript levels were determined by quantitative real-time PCR using SYBR green dye on an ABI PRISM 7700 sequence detection system (Applied Biosystems). Data were analyzed by the comparative $\Delta\Delta C_T$ method according to the manufacturer's instructions (ABI PRISM 7700 User Bulletin 2). Single-band PCR products were confirmed on an agarose gel.

SA Quantification

Leaf material (100 to 200 mg fresh weight) was extracted with aqueous methanol (Bednarek et al., 2005). Leaf extracts were hydrolyzed with β -glucosidase (EC 3.2.1.21; Sigma-Aldrich), and released SA was reextracted as described (Lee and Raskin, 1998). HPLC analyses were performed on an Agilent 1100 HPLC system.

Generation of Stable Transgenic Lines Expressing Wild-Type or Mutant *FMO1*

The *FMO1* coding region (without the stop codon) was amplified from *Arabidopsis* Col-0 cDNA using gene-specific primers (sequences available on request). Wild-type and mutant forms of *FMO1* in pENTR/D-TOPO were recombined into the expression vector pXCSG-Strep to generate an in-frame C-terminal fusion to the eight-amino acid StrepII affinity purification tag and transformed into *fmo1-1* plants as described previously (Witte et al., 2004). Independent, homozygous, single insertion lines were identified and analyzed for *FMO1*-StrepII expression by StrepII purification essentially as described by Witte et al. (2004). Leaf material (2.5 g) of 4-week-old *Arabidopsis* plants was extracted in 3.75 mL of Ex-strep buffer containing 0.2% Triton X-100 and 100 mM Tris-HCl, pH 8. Extracts were centrifuged at 18,000g and the supernatant incubated with StrepTactine Sepharose (IBA) for 1 h at 4°C. The resin was washed and protein eluted in 600 μ L of E buffer (10 mM Tris, pH 8.0, 10 mM desthiobiotin, 2 mM DTT, 0.05% Triton X-100, and 50 mM NaCl). The eluted fraction was incubated with 6 μ L of StrataClean resin (Stratagene) and the resin then boiled in 40 μ L SDS-PAGE sample buffer before loading onto 10% SDS-PAGE gels. Proteins were electroblotted to nitrocellulose membranes that were then incubated with StrepII-specific monoclonal antibody conjugated with horseradish peroxidase (IBA) followed by chemiluminescence detection (Pierce).

Sequence Alignments and Phylogenetic Analysis

Alignment of amino acid sequences was performed using ClustalX (version 1.8) (Thompson et al., 1997) and edited for display with GeneDoc (version 2.6.002) (Nicholas et al., 1997). Phylogenetic analysis of *Arabidopsis* Nudix hydrolase amino acid sequences was performed using MEGA3 (Kumar et al., 2004). A neighbor-joining tree was constructed using a p-distance amino acid distance model and complete deletion. Bootstrap values from 1000 replications are shown at the tree nodes. The alignment of the Nudix hydrolase sequences is shown in Supplemental Figure 3 online.

Accession Numbers

The accession numbers for the genes discussed in this article are as follows: *EDS1* (At3g48090), *PAD4* (At3g52430), *SID2* (At1g74710), *FMO1* (At1g19250, corrected open reading frame has been reported to TAIR and will be updated for the next annotation release), *NUDT6* (At2g04450), *NUDT7* (At4g12720), *ACTIN* (At3g18780), and *UBIQUITIN* (At4g05320). *Arabidopsis* Genome Initiative numbers for candidate genes from Groups I, II, and III are given in Table 2 and in Supplemental Tables 2 and 3 online, respectively. Proteins in the alignment shown in Figure 5A are as follows (GenBank accession or *Arabidopsis* Genome Initiative numbers are indicated in parentheses): *FMO1* (AAF82235), *YUCCA* (At4g32540), *Os FMO* (XP_470552), *bFMO* (AAM18566), *yFMO* (NP_012046), and *hFMO1* (NP_002012). Microarray data from this article have been deposited with the ArrayExpress data library (<http://www.ebi.ac.uk/arrayexpress/>) under accession number E-MEXP-546.

Supplemental Data

The following materials are available in the online version of this article.

Supplemental Table 1. Expression Data of 4333 Pathogen-Responsive Probe Sets.

Supplemental Table 2. DC3000/*avrRps4*-Induced Genes in an *EDS1*- and *PAD4*-Dependent Manner (30 Probe Sets/33 Genes; Group II).

Supplemental Table 3. Genes Suppressed in *eds1* and *pad4* in Untreated Tissue (20 Probe Sets/21 Genes; Group III).

Supplemental Figure 1. Characterization of Insertion Lines Corresponding to Candidate Genes with *EDS1/PAD4*-Dependent Expression.

Supplemental Figure 2. Plant Resistance Phenotypes in Response to Inoculation with Avirulent *H. parasitica* Isolate Emco5 (Recognized by *RPP8*) on Ler-0 Wild Type, *eds1-2*, *pad4-2*, and *fmo1-2*.

Supplemental Figure 3. Full Alignment of *Arabidopsis* Nudix Hydrolases.

ACKNOWLEDGMENTS

We thank Daniela Eggle in the Schultze laboratory for help with microarray data analysis, Marcel Wiermer for help generating Col *eds1-2*, and John Mundy and Murray Grant for useful discussions. We also thank the Alexander von Humboldt Foundation "Sofja Kovalesjaka" program (J.E.P.) and the International Max-Planck Research School (E.G.). This work was supported by grants from the Bundesministerium für Bildung und Forschung GABI-Trilateral Project "DILEMA" (M.B.).

Received December 1, 2005; revised February 3, 2006; accepted February 17, 2006; published March 10, 2006.

REFERENCES

- Aarts, N., Metz, M., Holub, E., Staskawicz, B.J., Daniels, M.J., and Parker, J.E. (1998). Different requirements for *EDS1* and *NDR1* by disease resistance genes define at least two *R* gene-mediated signaling pathways in *Arabidopsis*. *Proc. Natl. Acad. Sci. USA* **95**, 10306–10311.
- Bednarek, P., Schneider, B., Svatos, A., Oldham, N.J., and Hahlbrock, K. (2005). Structural complexity, differential response to infection, and tissue specificity of indolic and phenylpropanoid secondary metabolism in *Arabidopsis* roots. *Plant Physiol.* **138**, 1058–1070.
- Bektas, M., Akcakaya, H., Aroyamak, A., Nurten, F., and Bermek, E. (2005). Effect of oxidative stress on in vivo ADP-ribosylation of eukaryotic elongation factor 2. *Int. J. Biochem. Cell Biol.* **37**, 91–99.
- Belkhadir, Y., Subramaniam, R., and Dangl, J.L. (2004). Plant disease resistance protein signaling: NBS-LRR proteins and their partners. *Curr. Opin. Plant Biol.* **7**, 391–399.
- Benjamini, Y., and Hochberg, Y. (1995). Controlling the false discovery rate - A practical and powerful approach to multiple testing. *J. R. Stat. Soc. B* **57**, 289–300.
- Bessman, M.J., Frick, D.N., and O'Handley, S.F. (1996). The MutT proteins or "Nudix" hydrolases, a family of versatile, widely distributed, "housecleaning" enzymes. *J. Biol. Chem.* **271**, 25059–25062.
- Brodersen, P., Malinovsky, F.G., Hematy, K., Newman, M.A., and Mundy, J. (2005). The role of salicylic acid in the induction of cell death in *Arabidopsis acd11*. *Plant Physiol.* **138**, 1037–1045.
- Brodersen, P., Petersen, M., Pike, H.M., Olszak, B., Skov, S., Odum, N., Jorgensen, L.B., Brown, R.E., and Mundy, J. (2002). Knockout of *Arabidopsis ACCELERATED-CELL-DEATH11* encoding a sphingosine transfer protein causes activation of programmed cell death and defense. *Genes Dev.* **16**, 490–502.
- Choi, H.S., Kim, J.K., Cho, E.H., Kim, Y.C., Kim, J.I., and Kim, S.W. (2003). A novel flavin-containing monooxygenase from *Methylophaga* sp strain SK1 and its indigo synthesis in *Escherichia coli*. *Biochem. Biophys. Res. Commun.* **306**, 930–936.
- Coppinger, P., Repetti, P.P., Day, B., Dahlbeck, D., Mehler, A., and Staskawicz, B.J. (2004). Overexpression of the plasma

- membrane-localized NDR1 protein results in enhanced bacterial disease resistance in *Arabidopsis thaliana*. *Plant J.* **40**, 225–237.
- Davletova, S., Rizhsky, L., Liang, H.J., Zhong, S.Q., Oliver, D.J., Coutu, J., Shulaev, V., Schlauch, K., and Mittler, R.** (2005). Cytosolic ascorbate peroxidase 1 is a central component of the reactive oxygen gene network of *Arabidopsis*. *Plant Cell* **17**, 268–281.
- De Block, M., Verduyn, C., De Brouwer, D., and Cornelissen, M.** (2005). Poly(ADP-ribose) polymerase in plants affects energy homeostasis, cell death and stress tolerance. *Plant J.* **41**, 95–106.
- de Torres, M., Sanchez, P., Fernandez-Delmond, I., and Grant, M.** (2003). Expression profiling of the host response to bacterial infection: The transition from basal to induced defence responses in *RPM1*-mediated resistance. *Plant J.* **33**, 665–676.
- Dong, X.N.** (2004). NPR1, all things considered. *Curr. Opin. Plant Biol.* **7**, 547–552.
- Eulgem, T., Weigman, V.J., Chang, H.S., McDowell, J.M., Holub, E.B., Glazebrook, J., Zhu, T., and Dangl, J.L.** (2004). Gene expression signatures from three genetically separable resistance gene signaling pathways for downy mildew resistance. *Plant Physiol.* **135**, 1129–1144.
- Falk, A., Feys, B.J., Frost, L.N., Jones, J.D.G., Daniels, M.J., and Parker, J.E.** (1999). *EDS1*, an essential component of *R* gene-mediated disease resistance in *Arabidopsis* has homology to eukaryotic lipases. *Proc. Natl. Acad. Sci. USA* **96**, 3292–3297.
- Feys, B.J., Moisan, L.J., Newman, M.A., and Parker, J.E.** (2001). Direct interaction between the *Arabidopsis* disease resistance signaling proteins, *EDS1* and *PAD4*. *EMBO J.* **20**, 5400–5411.
- Feys, B.J., Wiermer, M., Bhat, R.A., Moisan, L.J., Medina-Escobar, N., Neu, C., Cabral, A., and Parker, J.E.** (2005). *Arabidopsis* SENESENCE-ASSOCIATED GENE101 stabilizes and signals within an ENHANCED DISEASE SUSCEPTIBILITY1 complex in plant innate immunity. *Plant Cell* **17**, 2601–2613.
- Fraaije, M.W., Kamerbeek, N.M., van Berkel, W.J.H., and Janssen, D.B.** (2002). Identification of a Baeyer-Villiger monooxygenase sequence motif. *FEBS Lett.* **518**, 43–47.
- Glazebrook, J.** (2005). Contrasting mechanisms of defense against biotrophic and necrotrophic pathogens. *Annu. Rev. Phytopathol.* **43**, 205–227.
- Glazebrook, J., Chen, W.J., Estes, B., Chang, H.S., Nawrath, C., Metraux, J.P., Zhu, T., and Katagiri, F.** (2003). Topology of the network integrating salicylate and jasmonate signal transduction derived from global expression phenotyping. *Plant J.* **34**, 217–228.
- Irizarry, R.A., Hobbs, B., Collin, F., Beazer-Barclay, Y.D., Antonellis, K.J., Scherf, U., and Speed, T.P.** (2003). Exploration, normalization, and summaries of high density oligonucleotide array probe level data. *Biostatistics* **4**, 249–264.
- Jirage, D., Tootle, T.L., Reuber, T.L., Frost, L.N., Feys, B.J., Parker, J.E., Ausubel, F.M., and Glazebrook, J.** (1999). *Arabidopsis thaliana* *PAD4* encodes a lipase-like gene that is important for salicylic acid signaling. *Proc. Natl. Acad. Sci. USA* **96**, 13583–13588.
- Kang, L.W., Gabelli, S.B., Cunningham, J.E., O'Handley, S.F., and Amzel, L.M.** (2003). Structure and mechanism of MT-ADPRase, a nudix hydrolase from *Mycobacterium tuberculosis*. *Structure* **11**, 1015–1023.
- Kolisek, M., Beck, A., Fleig, A., and Penner, R.** (2005). Cyclic ADP-ribose and hydrogen peroxide synergize with ADP-ribose in the activation of TRPM2 channels. *Mol. Cell* **18**, 61–69.
- Kubo, A., Itoh, S., Itoh, K., and Kamataki, T.** (1997). Determination of FAD-binding domain in flavin-containing monooxygenase 1 (FMO1). *Arch. Biochem. Biophys.* **345**, 271–277.
- Kumar, S., Tamura, K., and Nei, M.** (2004). MEGA3: Integrated software for molecular evolutionary genetics analysis and sequence alignment. *Brief. Bioinform.* **5**, 150–163.
- Lawton, M.P., et al.** (1994). A nomenclature for the mammalian flavin-containing monooxygenase gene family based on amino acid sequence identities. *Arch. Biochem. Biophys.* **308**, 254–257.
- Lee, H.I., and Raskin, I.** (1998). Glucosylation of salicylic acid in *Nicotiana tabacum* cv. Xanthi-nc. *Phytopathology* **88**, 692–697.
- Lipka, V., et al.** (2005). Pre- and postinvasion defenses both contribute to nonhost resistance in *Arabidopsis*. *Science* **310**, 1180–1183.
- Lorrain, S., Vaillau, F., Balaque, C., and Roby, D.** (2003). Lesion mimicking mutants: Keys for deciphering cell death and defense pathways in plants? *Trends Plant Sci.* **8**, 263–271.
- Maldonado, A.M., Doerner, P., Dixon, R.A., Lamb, C.J., and Cameron, R.K.** (2002). A putative lipid transfer protein involved in systemic resistance signalling in *Arabidopsis*. *Nature* **419**, 399–403.
- Mateo, A., Muhlenbock, P., Rusterucci, C., Chang, C.C.C., Miszalski, Z., Karpinska, B., Parker, J.E., Mullineaux, P.M., and Karpinski, S.** (2004). LESION SIMULATING DISEASE 1 is required for acclimation to conditions that promote excess excitation energy. *Plant Physiol.* **136**, 2818–2830.
- McDonald, L.J., Wainschel, L.A., Oppenheimer, N.J., and Moss, J.** (1992). Amino acid-specific ADP-ribosylation: Structural characterization and chemical differentiation of ADP-ribose cysteine adducts formed nonenzymatically and in a pertussis toxin-catalyzed reaction. *Biochemistry* **31**, 11881–11887.
- McLennan, A.G.** (1999). The MutT motif family of nucleotide phosphohydrolases in man and human pathogens (review). *Int. J. Mol. Med.* **4**, 79–89.
- Naumann, C., Hartmann, T., and Ober, D.** (2002). Evolutionary recruitment of a flavin-dependent monooxygenase for the detoxification of host plant-acquired pyrrolizidine alkaloids in the alkaloid-defended arctiid moth *Tyria jacobaleae*. *Proc. Natl. Acad. Sci. USA* **99**, 6085–6090.
- Nawrath, C., Heck, S., Parinthewong, N., and Metraux, J.P.** (2002). *EDS5*, an essential component of salicylic acid-dependent signaling for disease resistance in *Arabidopsis*, is a member of the MATE transporter family. *Plant Cell* **14**, 275–286.
- Nicholas, K.B., Nicholas, H.B., Jr., and Deerfield II, D.W.** (1997). GeneDoc: Analysis and visualization of genetic variation. *EMBnet. news* **4**, 1–4.
- Nürnberg, T., Brunner, F., Kemmerling, B., and Piater, L.** (2004). Innate immunity in plants and animals: Striking similarities and obvious differences. *Immunol. Rev.* **198**, 249–266.
- Ogawa, T., Ueda, Y., Yoshimura, K., and Shigeoka, S.** (2005). Comprehensive analysis of cytosolic Nudix hydrolases in *Arabidopsis thaliana*. *J. Biol. Chem.* **280**, 25277–25283.
- Olejnik, K., and Kraszewska, E.** (2005). Cloning and characterization of an *Arabidopsis thaliana* Nudix hydrolase homologous to the mammalian GFG protein. *Biochim. Biophys. Acta* **1752**, 133–141.
- Olszak, B., Malinovsky, F.G., Brodersen, P., Grell, M., Giese, H., Petersen, M., and Mundy, J.** (2006). A putative flavin-containing mono-oxygenase as a marker for certain defense and cell death pathways. *Plant Sci.* **170**, 614–623.
- Perraud, A.L., Fleig, A., Dunn, C.A., Bagley, L.A., Launay, P., Schmitz, C., Stokes, A.J., Zhu, Q.Q., Bessman, M.J., Penner, R., Kinet, J.P., and Scharenberg, A.M.** (2001). ADP-ribose gating of the calcium-permeable LTRPC2 channel revealed by Nudix motif homology. *Nature* **411**, 595–599.
- Perraud, A.L., Takanishi, C.L., Shen, B., Kang, S., Smith, M.K., Schmitz, C., Knowles, H.M., Ferraris, D., Li, W.X., Zhang, J., Stoddard, B.L., and Scharenberg, A.M.** (2005). Accumulation of free

- ADP-ribose from mitochondria mediates oxidative stress-induced gating of TRPM2 cation channels. *J. Biol. Chem.* **280**, 6138–6148.
- Redman, J.C., Haas, B.J., Tanimoto, G., and Town, C.D.** (2004). Development and evaluation of an *Arabidopsis* whole genome Affymetrix probe array. *Plant J.* **38**, 545–561.
- Rescigno, M., and Perham, R.N.** (1994). Structure of the NADPH-binding motif of glutathione reductase: Efficiency determined by evolution. *Biochemistry* **33**, 5721–5727.
- Richter, C., and Schlegel, J.** (1993). Mitochondrial calcium release induced by prooxidants. *Toxicol. Lett.* **67**, 119–127.
- Rustérucci, C., Aviv, D.H., Holt, B.F., Dangl, J.L., and Parker, J.E.** (2001). The disease resistance signaling components *EDS1* and *PAD4* are essential regulators of the cell death pathway controlled by *LSD1* in *Arabidopsis*. *Plant Cell* **13**, 2211–2224.
- Song, J.T., Lu, H., McDowell, J.M., and Greenberg, J.T.** (2004). A key role for *ALD1* in activation of local and systemic defenses in *Arabidopsis*. *Plant J.* **40**, 200–212.
- Suh, J.K., Poulsen, L.L., Ziegler, D.M., and Robertus, J.D.** (1999). Yeast flavin-containing monooxygenase generates oxidizing equivalents that control protein folding in the endoplasmic reticulum. *Proc. Natl. Acad. Sci. USA* **96**, 2687–2691.
- Sundaresan, V., Springer, P., Volpe, T., Haward, S., Jones, J.D.G., Dean, C., Ma, H., and Martienssen, R.** (1995). Patterns of gene action in plant development revealed by enhancer trap and gene trap transposable elements. *Genes Dev.* **9**, 1797–1810.
- Thompson, J.D., Gibson, T.J., Plewniak, F., Jeanmougin, F., and Higgins, D.G.** (1997). The CLUSTAL_X windows interface: Flexible strategies for multiple sequence alignment aided by quality analysis tools. *Nucleic Acids Res.* **25**, 4876–4882.
- Tobena-Santamaria, R., Bliet, M., Ljung, K., Sandberg, G., Mol, J.N.M., Souer, E., and Koes, R.** (2002). FLOOZY of petunia is a flavin mono-oxygenase-like protein required for the specification of leaf and flower architecture. *Genes Dev.* **16**, 753–763.
- Torres, M.A., Jones, J.D.G., and Dangl, J.L.** (2005). Pathogen-induced, NADPH oxidase-derived reactive oxygen intermediates suppress spread of cell death in *Arabidopsis thaliana*. *Nat. Genet.* **37**, 1130–1134.
- Wiermer, M., Feys, B.J., and Parker, J.E.** (2005). Plant immunity: The EDS1 regulatory node. *Curr. Opin. Plant Biol.* **8**, 383–389.
- Wildermuth, M.C., Dewdney, J., Wu, G., and Ausubel, F.M.** (2001). Isochorismate synthase is required to synthesize salicylic acid for plant defence. *Nature* **414**, 562–565.
- Witte, C.P., Noel, L.D., Gielbert, J., Parker, J.E., and Romeis, T.** (2004). Rapid one-step protein purification from plant material using the eight-amino acid StrepII epitope. *Plant Mol. Biol.* **55**, 135–147.
- Zhang, M., and Robertus, J.D.** (2002). Molecular cloning and characterization of a full-length flavin-dependent monooxygenase from yeast. *Arch. Biochem. Biophys.* **403**, 277–283.
- Zhao, Y.D., Christensen, S.K., Fankhauser, C., Cashman, J.R., Cohen, J.D., Weigel, D., and Chory, J.** (2001). A role for flavin monooxygenase-like enzymes in auxin biosynthesis. *Science* **291**, 306–309.
- Zhou, N., Tootle, T.L., Tsui, F., Klessig, D.F., and Glazebrook, J.** (1998). *PAD4* functions upstream from salicylic acid to control defense responses in *Arabidopsis*. *Plant Cell* **10**, 1021–1030.

NOTE ADDED IN PROOF

Identification of *NUDT7* (referred to as *GFG1*) was also reported by Jambunathan and Mahalingam (2005).

Jambunathan, N., and Mahalingam, R. (December 3, 2005). Analysis of *Arabidopsis Growth Factor Gene 1 (GFG1)* encoding a nudix hydrolase during oxidative signaling. *Planta* <http://dx.doi.org/10.1007/s00425-005-0183-y>.